Conformational Analysis, Pharmacophore Identification, and Comparative Molecular Field Analysis of Ligands for the Neuromodulatory σ_3 Receptor

Andrew M. Myers, Paul S. Charifson,† Constance E. Owens, Nora S. Kula,‡ Andrew T. McPhail,§ Ross J. Baldessarini,‡ Raymond G. Booth, and Steven D. Wyrick*

Division of Medicinal Chemistry and Natural Products, School of Pharmacy, CB No. 7360, University of North Carolina, Chapel Hill, North Carolina 27599-7360

Received May 12, 1994®

Molecular modeling studies were carried out on a series of 1-phenyl-3-amino-1,2,3,4-tetrahydronaphthalenes (phenylaminotetralins, PATs), several PAT structural analogs, and various non-PAT ligands that demonstrate a range of affinities for a novel σ_3 receptor linked to stimulation of tyrosine hydroxylase and dopamine synthesis in rodent brain. In an effort to develop a ligand-binding model for the σ_3 receptor, a pharmacophore mapping program (DISCO) was used to identify structural features that are common to ligands that exhibit moderate to high binding affinity for σ_3 sites. DISCO then was utilized to propose a common pharmacophoric region that included one low-energy conformation of each compound in the training set. The resulting alignment was utilized in a comparative molecular field analysis (CoMFA) study in an attempt to correlate the steric and electrostatic fields of the molecules with the respective binding affinities at the σ_3 receptor. A suitably predictive model was obtained from the CoMFA analysis which will be employed in the development of additional PAT analogs that could potentially display high affinity and selectivity for the σ_3 receptor. The excluded volumes which resulted from comparing molecular volumes of active and inactive compounds were visualized to examine the limits of steric tolerance imposed by the σ_3 receptor.

Introduction

The σ receptor once was believed to belong to the opioid class of receptors; however, subsequent examination has revealed a non-opioid pharmacology.[1,2] Efforts to fully characterize the σ receptor have been impeded because an endogenous σ ligand has not been identified nor has a σ-type receptor been isolated or cloned.[2] There is evidence that σ receptors may modulate catecholaminergic systems[3-7] and that σ receptors may be G-protein coupled.[2,8] Multiple σ receptor subtypes have been proposed,[8-10] and recently, it was agreed to classify those that bind the (+)-benzomorphans with high versus low affinity as σ_1 and σ_2, respectively.[2,9,10] Other novel functional receptors characterized in C6 glioma cells,[11] turtle brain,[12] clonal cell lines,[13] and NCB-20 cells[14] appear to be distinct from the σ_1 and σ_2 classes.

Several computational models and structure–activity relationships for σ receptor ligands have been developed in an effort to characterize σ binding sites and to find common structural features among σ receptor ligands.[15-20] These models have provided valuable insight into structural determinants that effect ligand binding to σ versus opioid,[15] phenylcyclidine (PCP),[16,17] and dopamine[18] receptors. More recently, Glennon and coinvestigators have identified structural elements that directly contribute to potent σ receptor binding and selectivity.[19,20] On the basis of SAR studies in which certain amine-substituted[19] and conformationally restricted[20] derivatives exhibited high affinity and selectivity for [^{3}H]DTG-labeled σ receptors, Glennon has proposed that the primary σ receptor pharmacophore consists of a substituted 1-phenyl-2-aminopropane moiety.

Recently, we reported that certain analogs in a series of 1-phenyl-3-amino-1,2,3,4-tetrahydronaphthalenes (1-phenyl-3-aminotetralins, PATs) bind stereoselectively and with high affinity to a σ-like site in rodent striatum which we propose as the σ_3 receptor and show negligible affinity for other known σ sites in addition to over two dozen other CNS recognition sites.[21,22] We also have demonstrated that σ_3 binding sites are linked to the modulation of tyrosine hydroxylase (TH) and dopamine (DA) synthesis in striatum. The most active PATs (**1** and **3**, Table 1) stimulate TH 30–40% above control levels at 0.1 μM.[21] This neuromodulatory effect is blocked by the σ antagonist BMY-14802. Preliminary structure–activity relationships[22] in this series revealed that there exists little steric tolerance regarding substituents on the amine nitrogen examined thus far (Table 1, **1**–**12**), with the dimethyl substitution producing the highest σ_3 receptor affinity. Of the aromatic substitutions examined thus far, the 6-chloro-7-hydroxy and unsubstituted analogs **3** and **1**, respectively, demonstrated comparable binding affinity. Catechol analogs **5** and **6** were found to be either functionally inactive or inhibitory with regard to striatal DA synthesis and also were found to possess reduced affinity for the σ-like site labeled by [^{3}H]-**3**.[23] Due to the more complicated pharmacological profile displayed by **3**, **5**, and **6**, our subsequent efforts have been directed toward the aryl-substituted analog **1**. Other PAT analogs have been synthesized (**13**–**17**) and evaluated for binding affinity (Table 1) in an effort to define the structural requirements for binding to the σ_3 receptor.[24] Separation of the enantiomers and X-ray crystallographic analysis of **1** have revealed that the greatest affinity for the σ_3 receptor resides in the 1*R*,3*S*-(−) isomer.[22] This stere-

* Person to whom all correspondences should be addressed. Tel: (919) 962-0075. FAX: (919) 966-6919.
† Glaxo Research Institute, 5 Moore Dr., Research Triangle Park, NC 27709.
‡ Mailman Research Center, McLean Division of Massachusetts General Hospital, Harvard Medical School, Belmont, MA 02178.
§ Department of Chemistry, Duke University, Durham, NC 27708.
® Abstract published in *Advance ACS Abstracts*, October 15, 1994.

0022-2623/94/1837-4109$04.50/0

Table 1. Conformational Data and Affinities of Phenylaminotetralins for the σ_3 Receptor

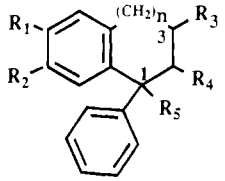

compd	config[a]	R_1	R_2	R_3	R_4	n	R_5	conformers[b]	ΔE[c]	pIC_{50}s[d]
(−)-**1**	*trans*	H	H	$N(CH_3)_2$	H	1	H	10	2.10	9.28
(+)-**1**	*trans*	H	H	$N(CH_3)_2$	H	1	H	11	0.73	8.35
2	*cis*	H	H	$N(CH_3)_2$	H	1	H	10	7.30	8.76
3	*trans*	Cl	OH	$N(CH_3)_2$	H	1	H	9	0.00	9.54
4	*cis*	Cl	OH	$N(CH_3)_2$	H	1	H	8	4.80	9.15
5	*trans*	OH	OH	$N(CH_3)_2$	H	1	H	9	0.00	7.77
6	*cis*	OH	OH	$N(CH_3)_2$	H	1	H	8	7.49	8.21
7	*trans*	H	H	$NH(CH_3)$	H	1	H	10	0.88	7.10
8	*trans*	Cl	OH	$NH(CH_3)$	H	1	H	10	0.41	7.98
9	*trans*	H	H	$N(C_2H_5)_2$	H	1	H	11	1.24	8.65
10	*trans*	H	H	$N(CH_3)C_3H_5$	H	1	H	12	1.94	8.35
11	*trans*	H	H	$NH(C_3H_5)$	H	1	H	12	2.27	7.23
12	*trans*	H	H	$N(C_3H_5)_2$	H	1	H	14	0.00	7.89
13	*trans*	H	H	H	$N(CH_3)_2$	1	H	8	5.99	6.02
14	*cis*	H	H	H	$N(CH_3)_2$	1	H	8	1.45	5.86
15	*trans*	H	H	$N(CH_3)_2$	H	1	CH_3	10	0.03	8.26
16	*trans*	H	H	$N(CH_3)_2$	H	2	H	18	2.97	7.76
17	*cis*	H	H	$N(CH_3)_2$	H	2	H	18	4.14	7.07

[a] Configuration (config) *cis* or *trans* denotes the relationship of substituents at positions 1 and 3. [b] Number of conformations found with energies within 10−12 kcal/mol above that of the lowest energy conformation found. [c] Energy difference between the DISCO conformer and the lowest energy conformation. [d] $-\log IC_{50}$ versus [^{3}H]-**3** or [^{3}H]-(−)-**1**.

oisomer has been radiolabeled and currently is being used to advance the pharmacological characterization of the σ_3 receptor.[25]

Here, we report the results of conformational analysis, pharmacophore identification, and comparative molecular field analysis (CoMFA) studies on the PAT series, as well as a variety of structurally diverse non-PATs that exhibit a broad range of binding affinities for the σ_3 receptor. The PATs included in the model development differ from one another regarding aryl substituents, N-substituents, size of the parent ring system, *cis* versus *trans* geometry relative to the C1 and C3 positions (Table 1), position of the amine group, and substituents at the 1-position of the tetralin ring. The non-PATs included in pharmacophore model development (Figure 1) represent ligands for a variety of CNS receptor classes. These include DA receptor ligands (**21**, **24**−**27**, **29**, **33**, **35**), 5-HT ligands (**20**, **22**, **23**, **28**, **30**), and σ_1/σ_2 ligands (**18**, **19**, **27**, **32**), in addition to ligands for adrenergic receptors (**31**) and cytochrome P_{450} enzymes (**34**). Since these compounds displayed high (**25**, **26**, **28**), intermediate (**20**, **21**, **24**), and modest (**18**, **19**, **22**, **23**, **27**, **29**−**33**) affinities (Table 2), a broad range of activities was utilized in the σ_3 receptor pharmacophore model development.

Results and Discussion

The goal of these computational studies was the development of a binding model which could accommodate the array of compounds that have affinity for the σ_3 receptor, if such a single model is possible. Whether a ligand interacts with its receptor in its global minimum energy conformation versus another similarly low-energy conformation is a question which must always be considered when modeling receptor interactions for flexible molecules. Therefore, representative low-energy conformers of each analog must be compared to representative low-energy conformers of all other analogs in order to elucidate a common alignment model which will accommodate all analogs. Martin has developed the program DISCO (DIStance COmparison)[26] for the purpose of identifying and systematically aligning common pharmacophoric elements among a series of flexible, structurally diverse analogs. The use of DISCO herein for alignment of the pharmacophoric regions represents one of the earliest external practical applications of this technique since its development. As such, the resulting models were derived by the intuitive manipulation of the DISCO program upon the basis of our previous experience with molecular modeling.[27−29] The results obtained from DISCO and subsequent CoMFA studies discussed below will be used for the design of additional PAT analogs with potentially high σ_3 receptor affinity and selectivity.

Conformational Analysis. In order to use the DISCO program to identify a potential pharmacophore for the σ_3 receptor, individual conformer databases were generated for all compounds. The Multisearch component of DISCO can be used to obtain these conformational databases. However, Multisearch parameters cannot presently be tailored to each molecular structure; therefore, we chose to search each analog independently (Tables 1 and 2). By using the Random Search and Grid Search features of SYBYL 6.0, molecular databases that represent a set of conformationally unique structures were developed for each training compound. The number of unique conformers in each database was regulated by a specified minimum rms (root mean square) deviation (0.2−1.0 Å) as well as an energy cutoff of 10−12 kcal/mol above that of the lowest energy conformer found in the search. This minimum rms value dictated that only energy-minimized conformers with rms fit deviations greater than that designated were included in the conformer database. This process effectively excluded those conformers that were not unique. The rms value used in each search was determined as a

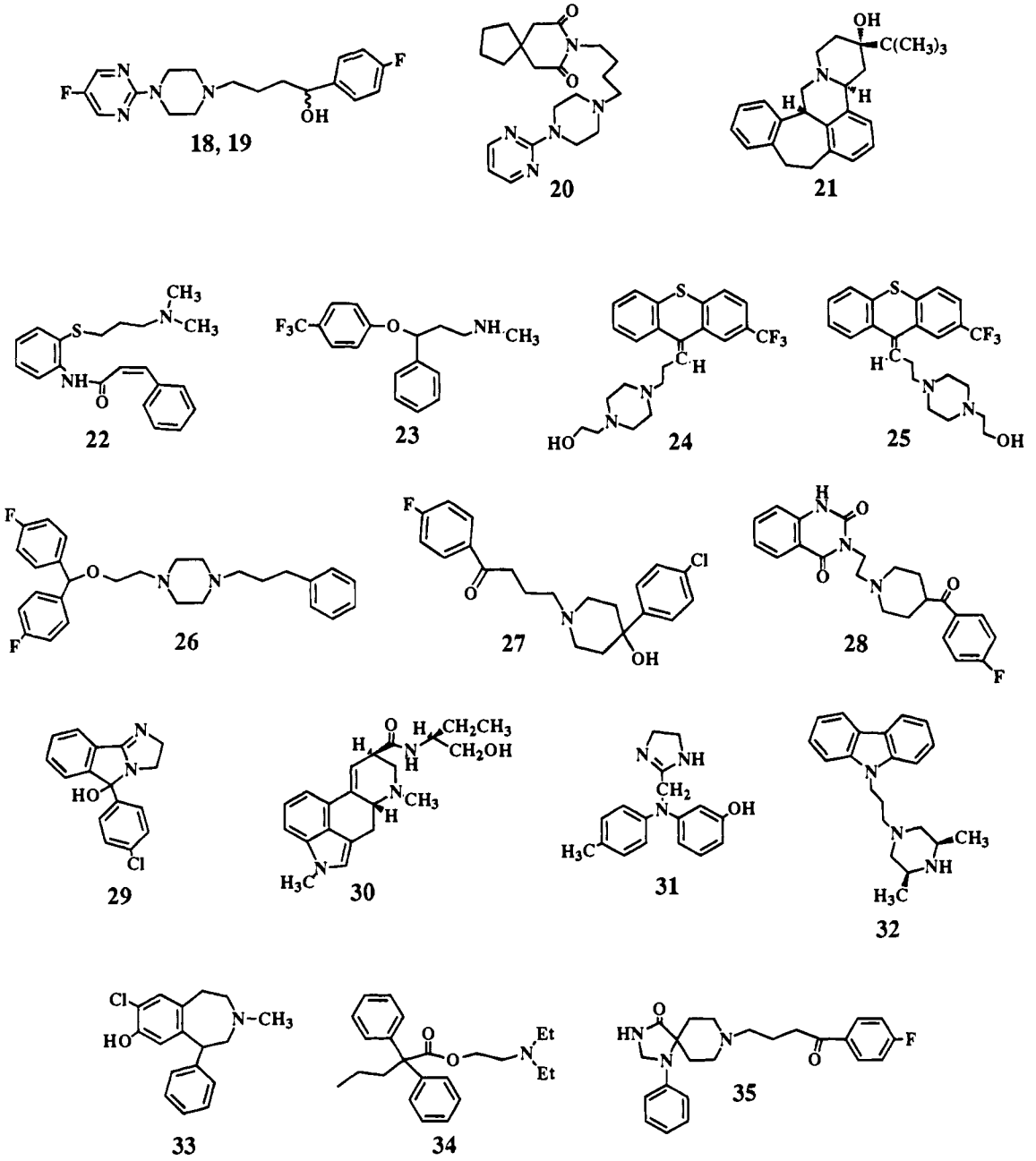

Figure 1.

function of the number of freely rotatable bonds that are present in each particular structure. For example, the rms value was set to a higher level (~1.0 Å) for those molecules with a large number of rotatable bonds (**20**, **22**, **26**–**28**, **35**) in order to limit large numbers of redundant conformers while at the same time adequately representing conformational space. Once the conformational databases were developed, a master database containing one conformer of each molecule in the evaluation set was utilized as a starting point for the DISCO program which is available as a module in the SYBYL 6.04 software.

DISCO Analysis. The first step of the DISCO search routine consists of identifying all potential pharmacophoric site points in each molecule of the master database. These site point assignments include aromatic and aliphatic ring centroids, functional groups with hydrogen bond donor potential (−OH, $-NH_2$, etc.), associated vector for the lone pairs of hydrogen bond acceptor groups (C=O, −OH, etc.), and external site points that represent receptor-associated hydrogen bond acceptors. The identical site points were then transferred to every conformer in each of the respective search databases. Before beginning the pharmacophore search, the 3-dimensional (x,y,z) coordinates of the conformer site points were recorded in a rms file which was obtained by comparing the coordinates of each conformer in a particular database to the "parent" conformer contained in the master database. This rms file was recalled for successive searches.

In order for a common pharmacophoric arrangement to be proposed by DISCO, a template molecule was chosen as the basis for site point comparison. This may be performed automatically by DISCO; however, we chose to designate the lead compound (1*R*,3*S*)-(−)-**1** as the template due to this analog's high affinity and selectivity for the σ_3 receptor (Table 1) and because of its less complex pharmacology.[21] Because of its high affinity, it was felt that the arrangement of pharmacophoric points for (−)-**1** would best represent that

Table 2. Conformational Data and Affinities of Non-PATs for the σ_3 Receptor

compound	conformers[a]	ΔE[b]	pIC_{50}[c]
18 (*R*)-BMY14802	33	9.78	6.36
19 (*S*)-BMY14802	34	10.17	6.67
20 buspirone	61	5.79	7.44
21 (+)-butaclamol	15	9.66	7.28
22 cinanserin	52	4.95	6.74
23 fluoxetine	39	7.14	6.07
24 *trans*-flupenthixol	35	2.61	7.83
25 *cis*-flupenthixol	35	4.14	8.65
26 GBR12909	72	11.65	9.00
27 haloperidol	39	9.90	6.67
28 ketanserin	28	3.02	9.00
29 mazindol	8	0.84	6.63
30 methylsergide	14	8.06	6.04
31 phentolamine	16	1.77	6.26
32 rimcazole	20	9.49	6.23
33 SCH23390	17	2.35	6.41
34 SKF525A	24	0.37	5.80
35 spiperone	33	9.07	6.02

[a] Number of conformations found with energies within 10–12 kcal/mol above that of the lowest energy conformation found. [b] Energy difference between the conformer used in DISCO and the lowest energy conformer. [c] $-\log IC_{50}$ versus [^{3}H]-**3** or [^{3}H]-(−)-**1**.

which was optimal for interaction with the σ_3 receptor. During each attempt, DISCO compared the coordinates of the site points assigned to the template conformer to the site point coordinates found in all of the other conformer databases. The site point comparison process was then repeated for each template conformer, resulting in the identification of one conformation of each analog that could be fitted to the template molecule within a designated tolerance level (Å).

By utilizing DISCO, a binding model was found that included all of the training compounds (Tables 1 and 2) fitted to four distinct pharmacophoric site points (two aromatic centroids, a hydrogen bond donor (protonated amine), and a receptor-associated hydrogen bond acceptor) within a tolerance of 2.8 Å. In DISCO, the tolerance level corresponds to the maximum allowable rms deviation for the fitted site points of each compound to the template. Few compounds had site point rms fit values that approached the 2.8 cutoff, and the average value for the final models was within the range of 0.752–1.25 Å. This tolerance level was chosen as the minimum value which would accommodate all of the molecules in the training set. In other DISCO analyses, stricter tolerances were utilized; however, these values lead to exclusion of certain non-PATs while not significantly affecting the overall alignment. The initial DISCO evaluation resulted in a total of 10 models, with one model associated with each conformer of the template database. The selection of an appropriate DISCO model involved the systematic elimination of models on the basis of inspection of the alignment of the compounds and on results obtained from subsequent CoMFA analyses. It was assumed that a pharmacologically relevant DISCO model would be associated with an initial positive cross-validated (cv) R^2 (q^2) when considering the entire training set. This assumption was used as an initial screening process whereby each DISCO model was subjected both to AutoCoMFA analysis (5 cv groups) and subsequently to a "leave-one-out" cross-validation analysis (36 cv groups).

The results from these preliminary CoMFA analyses are listed in Table 3. During the selection procedure,

Table 3. DISCO Model Evaluation

model (36 cv)	q^2 AutoCoMFA (5 cv groups)	q^2 CoMFA (36 cv groups)	Δ in q^2 (5 cv vs 36 cv)
A	−0.276	0.021	0.297
B	−0.057	−0.004	0.053
C	−0.307	0.012	0.319
D	−0.196	−0.103	0.093
E	−0.092	−0.083	0.009
F	−0.176	0.141	0.317
G	−0.126	0.164	0.290
H	−0.099	0.063	0.162
I	−0.118	0.181	0.299
J	−0.227	−0.266	−0.039

all models that resulted in negative q^2 values (36 cross-validation groups) were excluded from further consideration. Generally, those models with $q^2 > 0$ (A, C, F, G, H, I) were used for further CoMFA investigation. These six DISCO models were then inspected visually in an effort to eliminate models that may not represent an intuitively rational molecular alignment. The two models with weakest correlations, A and C, were subsequently eliminated because certain phenylaminotetralin analogs aligned with the template molecule [(−)-**1**] in an inverted manner. Specifically, the two PAT aromatic centroids were aligned to opposite points on the template. Since a common pharmacophoric alignment for the PAT-type ligands (**1**–**17**) is assumed, this alignment was deemed improbable and, in fact, may account for the low q^2 value (<0.050) calculated for each model. Models F and H were also eliminated due to the unexpected alignment of several compounds including **21**, **26**, **29**, and **30**. The elimination of model I was based on the alignment of both BMY-14802 isomers (**18** and **19**) with the template. In this model, DISCO aligned the nonaromatic piperazine rings of **18** and **19** with the aromatic site points, thus extending the terminal phenyl rings of **18** and **19** significantly beyond the steric region as defined by the remaining 34 compounds.

Close inspection revealed that model G appeared to represent the most rational alignment when considering the structural diversity of all **36** compounds in the training set. In this model, all of the PATs (**1**–**17**) were aligned in a similar manner, with none of the structural features of other compounds (**18**–**36**) extending beyond the steric region defined by the majority of conformers defining the model. The molecular alignment and pharmacophoric site points of model G are shown in Figure 2, and the energies of each conformer, selected for this alignment, relative to the lowest energy conformer found in the conformational search procedure, are listed in Tables 1 and 2. An overlay of the conformer of (−)-**1** (Figure **3**) that serves as a template for this model onto the corresponding X-ray crystal structure of its primary amine precursor[22] shows that both conformers possess a pseudoaxial 1-phenyl substituent and an equatorial 3-dimethylamino substituent. Ring B of the tetralin system prefers a half-chair conformation similar to that observed for the tetrahydroisoquinoline D_1 DA receptor antagonists.[27,29] Pertinent torsion angles for this template conformation are listed in Table 4.

CoMFA Analysis. Once model G was chosen from the DISCO results as the most appropriate pharmacophore alignment, a comprehensive CoMFA analysis

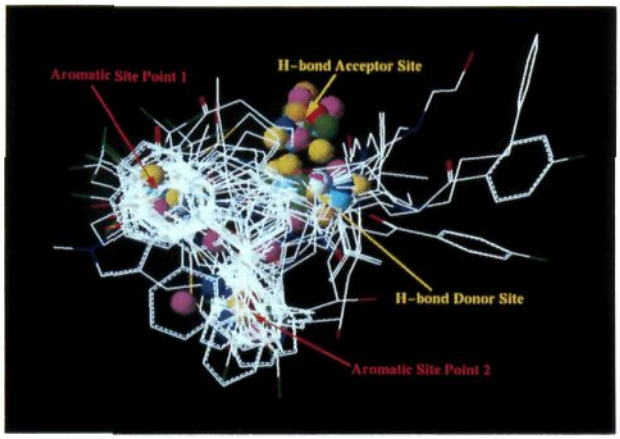

Figure 2.

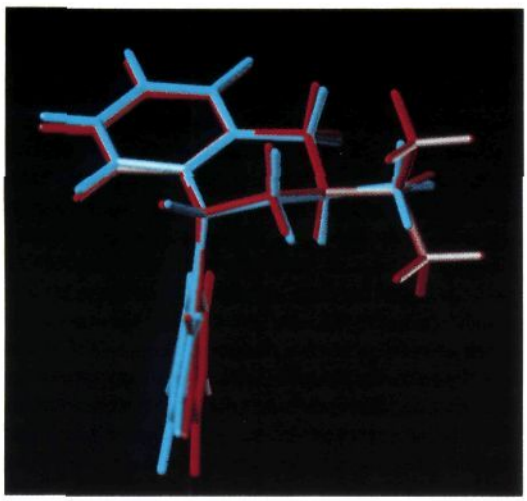

Figure 3.

Table 4. Torsion Angles (deg) Characterizing the Conformation of the DISCO Template

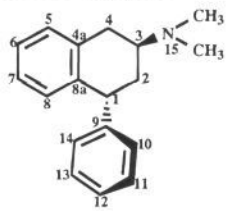

(1R,3S)-(−)-**1**

torsion angle[a]	calculated	X-ray[b]
C1−C2−C3−C4	66.5	64.8(3)
C1−C2−C3−N15	−166.1	−174.4(2)
C2−C1−C9−C10	77.3	70.0(3)
C3−C2−C1−C9	74.8	79.5(3)
C4a−C4−C3−N15	−176.6	−168.5(2)
C4a−C4−C3−C2	−48.8	−46.9(3)
C4a−C8a−C1−C9	−107.5	−109.8(3)
C8a−C1−C2−C3	−49.8	−48.9(3)
C8a−C1−C9−C10	−158.1	−161.6(3)

[a] The torsion angle A−B−C−D is defined as positive if, when viewed along the B−C bond, atom A must be rotated clockwise to eclipse atom D. [b] 1-(*R*)-(−)-Camphor-10-sulfonic acid salt (ref 22); values in parentheses are estimated standard deviations.

was initiated. A summary of the numerical results from these CoMFA studies is listed in Table 5. As stated above, "leave-one-out" cross-validation was used so that each compound would be systematically excluded and its activity predicted by the analysis during formulation of the regression equation. Following each analysis, assuming that an acceptable q^2 (i.e., >0.5) was obtained, a second PLS analysis was performed using the optimum number of components (as determined by weighting the q^2 versus the standard error of prediction (PRESS) value) with no cross-validation. Once a suitable CoMFA model was obtained, the accuracy of the non-cross-validated CoMFA-generated predictions was assessed by observing the resulting residuals (Table 6, Figure 4).

The process of developing a suitable CoMFA model required the evaluation of various training sets (Table 5) utilizing both cross-validated and non-cross-validated methods. In certain CoMFA training sets, one or more compounds were systematically eliminated from the analysis with subsequent analysis of the correlation. Also, both the default 2.0 Å grid spacing (Table 5, analyses 1−18) and the 1.0 Å grid spacing were used to define the CoMFA regions. It was found, however, that neither the 1.0 Å grid nor a −1 charged probe atom improved the correlation. Therefore, we chose to use the default grid and a positive probe atom for all subsequent analyses. The initial training sets analyzed employed the molecular alignment as proposed from the DISCO model and resulted in a positive correlation (q^2 = 0.261, PRESS = 0.979). The alignment presented by DISCO was then enhanced by "field fitting" (rigid) the molecular set to the chosen template [(−)-**1**] using the calculated electrostatic and steric fields associated with each molecule. In doing so, the steric and electrostatic fields of each molecule were aligned with those of the template so as to afford maximal overlap without altering the conformation. Analysis of this field-fitted alignment resulted in a q^2 = 0.352 (PRESS = 0.931). This represented a significant improvement over the result obtained solely on the basis of the DISCO alignment but was still below the threshold q^2 value of 0.5 which is considered to be minimal for a significantly internally predictive model.[30] All subsequent analyses utilized the field-fitted alignment as the basis for the molecular orientation of all 36 compounds. Comparison with results obtained by using the "field fit with minimization" alignment technique resulted in a diminished q^2 value. This approach allows for conformational change in order to allow for maximal field overlap with subsequent relaxation to a local minimum.

Our initial efforts to improve the statistical significance of the field-fitted analysis focused on the elimination of certain compounds with large residuals (i.e., ±1.5) when comparing experimentally determined (actual) pIC_{50}s to the predicted pIC_{50}s from CoMFA. These "poorly fitted" compounds included two *cis* PATs (**2** and **4**) and ketanserin (**28**). Several cross-validated analyses in which one or more of these compounds were dropped (analyses 9, 11, and 13) showed significant increases in q^2 values to a maximum of 0.655 when all three compounds were excluded from the analysis. Since **28** represented one of the compounds with highest affinity, it was difficult to rationalize its exclusion.

The general conclusion drawn from these studies was that those compounds that are predictive outliers from the first CoMFA analysis, especially the *cis* analogs **2** and **4**, serve to diminish the q^2 value generated by CoMFA. As a result of excluding certain of these

Table 5. CoMFA Results from DISCO Alignment Model G

analysis	observations omitted	alignment method	no. of cv groups	no. of comp	$(q^2/R^2)^a$	PRESS or std error[b]	F value	probability of $R^2 = 0$
AutoCoMFA	none	DISCO	5	5	0.030	1.640		
1	none	DISCO	36	5	0.261	0.979		
2	none	field fit	36	5	0.352	0.931		
3	none	field fit	0	5	0.920	0.337	78.5	0.017
4	none	field fit	0	4	0.790	0.530	65.7	0.056
5	**29**	field fit	35	5	0.381	0.899		
6	**5**	field fit	35	5	0.367	0.934		
7	**5, 6**	field fit	34	5	0.339	0.964		
9	**2, 4**	field fit	34	5	0.605	0.734		
10	**2, 4**	field fit	0	4	0.943	0.278	93.4	0.000
11	**2, 28**	field fit	34	5	0.498	0.818		
12	**2, 28**	field fit	0	4	0.935	0.300	80.5	0.000
13	**2, 4, 28**	field fit	33	5	0.655	0.673		
14	**2, 4, 28**	field fit	0	5	0.940	0.280	84.9	0.000
15	**2, 4, 6, 14, 17**	field fit	31	5	0.602	0.746		
16	**2, 4, 6, 14, 17**	field fit	0	5	0.947	0.272	89.2	0.000
17	**2, 4, 6, 14, 17, 28**	field fit	30	5	0.643	0.694		
18	**2, 4, 6, 14, 17, 28**	field fit	0	5	0.944	0.276	80.6	0.000

[a] q^2 represents cross-validated R^2 for analyses (AutoCoMFA 2, 5–9, 11, 13, 15, and 17), while R^2 represents the correlation coefficient for non-cross-validated PLS analyses (3, 4, 10, 12, 14, 16, and 18). [b] PRESS represents the standard error of prediction for cross-validated analyses (AutoCoMFA 2, 5–9, 11, 13, 15, and 17), while std error represents that for non-cross-validated PLS analyses (3, 4, 10, 12, 14, 16, and 18).

Table 6. Predicted pIC_{50}s and Residuals from CoMFA Analysis.

compd[a]	pIC_{50} actual	pIC_{50} predicted	residual
(−)-**1**	9.28	8.61	0.67
(+)-**1**	8.35	8.47	−0.12
3	9.54	8.86	0.68
5	7.77	8.40	−0.63
6	8.21	8.39	−0.18
7	7.10	7.59	−0.49
8	7.98	7.86	0.12
9	8.65	8.68	−0.03
10	8.35	8.30	0.04
11	7.23	7.30	−0.07
12	7.89	8.13	−0.24
13	6.02	6.16	−0.14
14	5.86	6.09	−0.23
15	8.26	8.32	−0.06
16	7.76	7.60	0.16
17	7.07	6.76	0.31
18	6.36	6.24	0.12
19	6.67	6.65	0.02
20	7.32	7.40	−0.08
21	7.28	7.39	−0.11
22	6.74	6.50	0.24
23	6.07	5.90	0.17
24	7.83	7.97	−0.14
25	8.65	8.56	0.09
26	9.00	9.03	−0.03
27	6.67	6.57	0.10
28	9.00	9.10	−0.10
29	6.63	6.63	−0.00073
30	6.04	6.28	−0.24
31	6.26	6.34	−0.08
32	6.23	6.06	0.17
33	6.41	6.27	0.14
34	5.80	5.80	0.0048
35	7.21	7.29	−0.08

[a] Compounds **2** and 4 were excluded from the analysis.

compounds, four models (analyses 9, 13, 15, and 17) were found that indicate a high degree of internal predictability ($q^2 > 0.600$) of the receptor affinities on the basis of steric and electrostatic characteristics. We felt that the best CoMFA results were obtained from analysis 9 which gave a $q^2 = 0.605$ with the number of optimal components equal to 5. The q^2 and standard error values, respectively, for each of the five components are as follows: component **1** = 0.284 and 0.924; component 2 = 0.459 and 0.816; component 3 = 0.549 and 0.757; component 4 = 0.592 and 0.732; component 5 = 0.605 and 0.734. The q^2 and standard error values for a 10-component model are 0.528 and 0.885. Analysis 9 was chosen since it accommodated the largest number of compounds (34) and because the exclusion of the two *cis* compounds (**2** and 4) can be rationalized because these specific compounds are functional antagonists at the σ_3 receptor and even though the agonist and antagonist sites are assumed to overlap, they may involve a different mode of binding not accurately represented by the model. Prior to the conformational search procedure described above, atomic charges had been calculated by the Gasteiger–Marsilli method (see the Experimental Section). Comparison to results obtained using AM1 charges revealed no significant differences between the two models in that the latter afforded a $q^2 = 0.611$. The numerical results of a non-cross-validated PLS analysis using the 34 compounds are listed in Table 6, and a plot of the predicted versus actual pIC_{50} are shown in Figure 4. The results from this analysis indicated a significant correlation ($R^2 = 0.943$), a small standard error (0.278), and a statistically insignificant probability of a spurious correlation ($p = 0.000$). The steric contribution was 69.8% while the

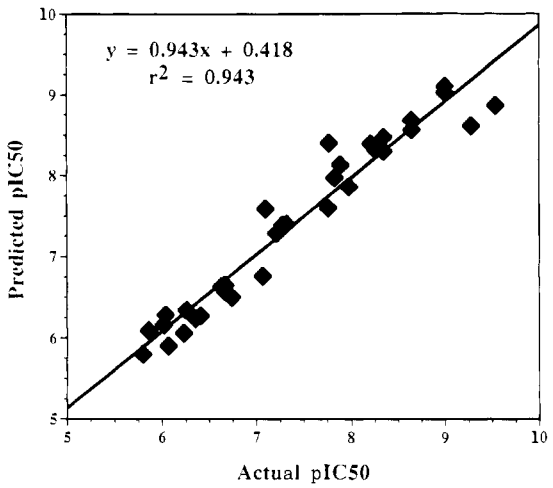

Figure 4.

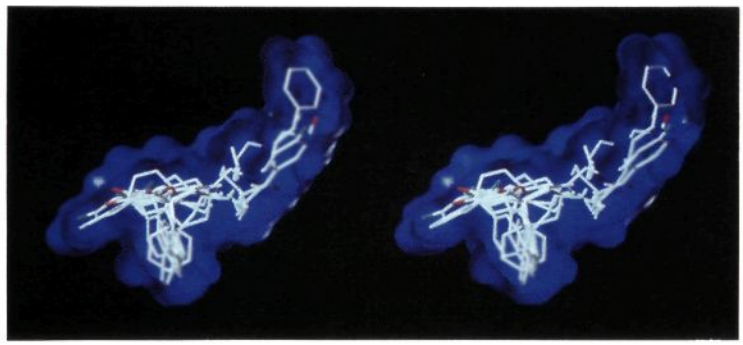

Figure 5.

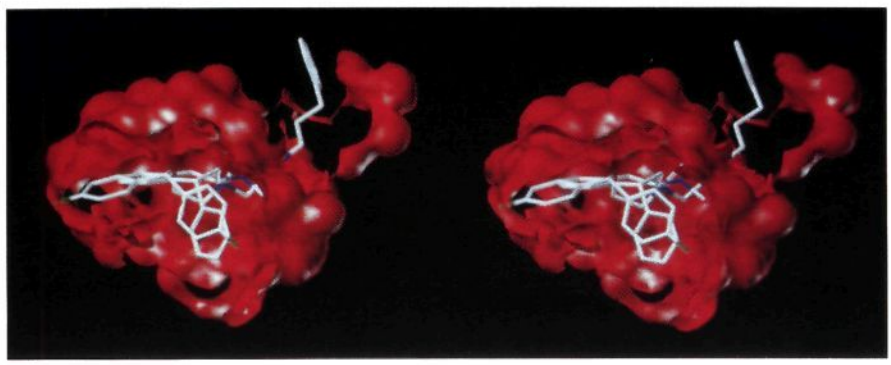

Figure 6.

electrostatic contribution was 30.2%. Steric contour grids generated from CoMFA generally agreed with the ligand-accessible and ligand-excluded volumes described below and shown in Figures 5 and 6 and are not shown since essentially no additional qualitative information is afforded relative to the volume representations.

Volume Representations. The steric volumes of the molecules used in the final CoMFA analysis were visualized through the use of Boolean volumetric representations of the field-fitted conglomerate generated via the mVolume option of SYBYL. Visualization of the volumes that contribute to the binding affinities of the active ($pIC_{50}s \geq 8.26$; Figure 5) versus less active ($pIC_{50}s \leq 7.98$; Figure 6) compounds indicates specific regions for high-affinity binding to the σ_3 receptor. As reported for high-affinity σ_1 ligands,[31] there appears to be an auxiliary binding region that can accommodate large (arylalkyl)amino substituents such as those associated with **26** and **28** within the domain of the σ_3 receptor. This region can be visualized as the additional volume that encompasses the N-substituents of the active compounds in Figure 5. A superimposition of **26** with (−)-**1** within the "ligand-excluded space" (Figure 6) more clearly illustrates this auxiliary binding region as an extended pocket in the receptor.

When comparing the above model to the Glennon σ_1/σ_2 proposed pharmacophore model,[19,20] similarities are noted with regard to the apparent auxiliary binding pocket which accommodates phenylalkyl nitrogen substituents as described above as well as the presence of at least one aromatic ring which need not be substituted. In contrast, Glennon proposes that the minimum σ_1/σ_2 pharmacophore consists of a 1-phenyl-2-aminopropane moiety or aminotetralin moiety. The DISCO/CoMFA model allows for a less moiety-dependent pharmacophore in that a variety of non-aminotetralins as well as non-1-phenyl-2-aminopropane-type compounds with adequate flexibility may assume low-energy conformations which will align with the pharmacophoric elements of two aromatic hydrophobes and a hydrogen bond-donating protonated amine. The primary structural feature which distinguishes the σ_3 pharmacophore from the σ_1/σ_2 appears to be the necessity for a second aromatic site point.

In summary, subsequent to extensive conformational searches within a finite energy window, the modeling software DISCO was used to systematically compare low-energy conformations of the PATs, PAT analogs, and structurally diverse non-PATs in order to identify a common pharmacophore and elucidate a common binding model. This model served as a suitable mode of alignment which was then enhanced by field fitting for subsequent CoMFA analyses. Elimination of two functional antagonists from the initial CoMFA model of choice resulted in a model with significant internal predictability that correlated the steric and electrostatic characteristics of 34 ligands with their affinities for the neuromodulatory σ_3 receptor. This model should aid in the design of additional ligands which possess high affinity and selectivity for this novel receptor as opposed to the σ_1/σ_2 receptor.

Experimental Section

All of the modeling techniques described herein were performed on either IBM Risc6000, Evans and Sutherland (ESV), or Silicon Graphics RS4000 Indigo workstations using the SYBYL 6.0 or 6.04 molecular modeling software from TRIPOS Associates, St. Louis, MO.

Conformational Analyses and DISCO Model Development. Construction of each PAT analog was based upon the 3-dimensional X-ray crystal coordinates of the *trans*-(1*R*,3*S*)-(−)-1-phenyl-3-amino-1,2,3,4-tetrahydronaphthalene precursor[22] to **1** as an input template for SYBYL 6.0. All other non-PAT compounds were constructed *de novo* using the sketch option of the building component of SYBYL 6.0. The analogs

were modeled as the protonated cationic amines as these analogs exist primarily in this form at pH 7.4 and it is assumed that the cationic amine group acts as a hydrogen bond donor at the σ_3 receptor. Charges for each structure were calculated using the Gasteiger–Marsilli method, and each analog was geometry optimized using the standard TRIPOS force field to an energy difference of 0.001 kcal/mol.

Conformational databases were developed for each compound using either the Random Search or Grid Search evaluation subroutines of SYBYL 6.0. In each case, the energy cutoff for conformers was designated as 10–12 kcal/mol above that of the lowest energy conformer found. Each search resulted in a molecular database that was representative of the conformational space that each analog occupies within the specified energy window. A master database containing one conformer for each molecule in the evaluation set was utilized as a starting point for the DISCO program which is available as a module in the SYBYL 6.04 software. The DISCO algorithm was used to find multipoint pharmacophoric models that illustrate common structural alignments for all compounds. This strategy resulted in several four-point pharmacophore models, each of which included one conformation from each molecular database. Several three- and five-point models were also considered and found to afford no additional information relative to the four-point models obtained.

Comparative Molecular Field Analysis (CoMFA).[30,32] Each model obtained from the DISCO analysis (see Results and Discussion) was used to initiate an AutoCoMFA study in order to correlate steric and electrostatic fields of each molecule with its binding affinity at the σ_3 receptor. AutoCoMFA used a partial least squares (PLS) algorithm with five components and five cross-validation groups. Subsequent CoMFA analyses for the selected model were performed using a number of cross-validation groups equal to the number of observations included. The DISCO alignment was enhanced by field fitting (rigid) the conformers in the model to the template in order to maximize the steric and electrostatic field overlap. The best analysis was then repeated without cross-validation and the resulting equation used for the internal prediction of the activities of the observations. CoMFA fields were calculated within the QSAR module of SYBYL 6.0. The steric (van der Waals interaction) and electrostatic (Coulombic values with a $1/r$ distance-dependent dielectric function) potential energy fields were calculated at each lattice intersection on a regularly spaced grid. The grid spacing was 2.0 Å in each direction, with the grid extending 26 Å in the x and y dimensions and 20 Å in the z dimension. For the higher corner of the region, x = 14.153, y = 13.697, and z = 9.009. For the lower corner, x = 11.658, y = 11.265, and z = 10.384. An sp^3 carbon atom with a van der Waals radius of 1.52 Å and a 1.0 charge was used as a probe atom for the calculations. Column filtering was equal to 2.0 kcal. Visualization of steric contours (not shown) that contribute to the binding affinities of the active versus less active compounds was achieved by obtaining steric grid maps from the distribution of the steric field generated for the CoMFA model.

Volume Representations. The field-fitted DISCO model utilized for the final CoMFA studies was also used for the determination of excluded and accessible receptor volume in which Boolean volumetric representations were generated using the mVolume routine of SYBYL 6.04. A volume was calculated for analogs ($pIC_{50} \geq 8.26$) which allowed for the description of the "ligand-accessible space". The ligand-accessible space was then subtracted from that of the less active analogs ($pIC_{50} < 7.98$) to afford the "ligand-excluded space" which is receptor occupied and is, therefore, inaccessible for ligand binding.

Acknowledgment. This work was supported by University of North Carolina Research Grants 5-44339 and 6-69410, USPHS Grants MH-31154, MH-34006, MH-47370, and MH40537, and an award from the Bruce J. Anderson Foundation. The authors wish to thank Dr. Chris Waller for technical assistance with the CoMFA analyses. The authors also wish to acknowledge the Laboratory for Molecular Modeling, Division of Medicinal Chemistry and Natural Products, School of Pharmacy, University of North Carolina at Chapel Hill. The authors thank Tripos and Associates for the generous provision of SYBYL 6.0 used for various phases of this work.

References

(1) Martin, W. R.; Eades, C. G.; Thomson, J. A.; Happler, R. E.; Gilbert, P. The effects of morphine and nalorphine-like drugs in the nondependent and morphine-dependent chronic spinal dog. *J. Pharmacol. Exp. Ther.* **1976**, *197*, 517–532.
(2) Walker, J. M.; Bowen, W. D.; Walker, F. O.; Matsumoto, R. R.; de Costa, B.; Rice, K. C. Sigma receptors: biology and function. *Pharmacol. Rev.* **1990**, *42*, 355–402.
(3) Gundlach, A. L.; Largent, B.; Snyder, S. H. Autoradiographic localization of sigma receptor binding sites in guinea pig central nervous system with (+)-[^{3}H]-(3-hydroxyphenyl)-N-(1-propyl)-piperidine. *J. Neurosci.* **1986**, *6*, 1757–1770.
(4) Campbell, B. G.; Bobker, D. H.; Leslie, F. M.; Mefford, I. N.; Weber, E. Both the signa receptor-specific ligand (−)-3-PPP and the PCP receptor-specific ligand TCP act in the mouse vas deferens via augmentation of electrically evoked norepinephrine release. *Eur. J. Pharmacol.* **1987**, *138*, 447–449.
(5) Arbilla, J. S.; Langer, S. Z. Differential effects of the stereoisomers of 3-PPP on dopaminergic and cholinergic neurotransmission in superfused slices of the corpus striatum. *Naunyn-Schmiedebergs Arch. Pharmacol.* **1984**, *327*, 6–13.
(6) Wachtel, S. R.; White, F. J. Electrophysiological effects of BMY-14802, a new potential antipsychotic drug, on midbrain dopamine neurons in the rat: acute and chronic studies. *J. Pharmacol. Exp. Ther.* **1988**, *244*, 410–416.
(7) Steinfels, G. F.; Tan, W. S. Selective sigma receptor agonist and antagonist affect dopamine neuronal activity. *Eur. J. Pharmacol.* **1989**, *163*, 167–170.
(8) Itzhak, Y.; Stein, I. Regulation of sigma receptors and responsiveness to guanine nucleotides following repeated exposure of rats to haloperidol: further evidence for multiple sigma binding sites. *Brain Res.* **1991**, *566*, 166–172.
(9) Quirion, R.; Bowen, W. D.; Itzhak, Y.; Junien, J. L.; Musacchio, J. M.; Rothman, R. B.; Su, T. P.; Tam, S. W.; Taylor, D. P. A proposal for the classification of sigma binding sites. *Trends Pharmacol. Sci.* **1992**, *13*, 85–86.
(10) Itzhak, Y.; Stein, I. Sigma binding sites in the brain: An emerging concept for multiple sites and relevance for psychiatric disorders. *Life Sci.* **1990**, *47*, 1073–1081.
(11) Vilner, B. J.; Bowen, W. D. Sigma receptor-active neuroleptics are cytotoxic to C6 glioma cells in culture. *Eur. J. Pharmacol.* **1993**, *244*, 199–201.
(12) Matsumoto, R. R.; Bowen, W. D.; de Costa, B. R.; Houk, J. A novel sigma binding site that may negatively modulate excitatory amino acid neurotransmission. *Soc. Neurosci. Abstr.* **1992**, *18*, 22.
(13) Vilner, B. J.; de Costa, B. R.; Bowen, W. D. Characterization of a novel sigma-like binding site for [^{3}H]-(+)-pentazocine in clonal cell lines. *Soc. Neurosci. Abstr.* **1992**, *18*, 22.
(14) Wu, X. Z.; Bell, J. A.; Spivak, C. E.; London, E. D.; Su, T. P. Electrophysiological and binding studies on intact NCB-20 cells suggest the presence of a low affinity sigma receptor. *J. Pharmacol. Exp. Ther.* **1991**, *257*, 351–359.
(15) Largent, B. L.; Wikström, H.; Gundlach, A.; Snyder, S. H. Structural determinants of sigma receptor affinity. *Mol. Pharmacol.* **1987**, *32*, 772–784.
(16) Manallack, D. T.; Beart, P. M. Quantitative conformational analyses predict distinct receptor sites for PCP-like and σ drugs. *Eur. J. Pharmacol.* **1987**, *144*, 231–235.
(17) Manallack, D. T.; Wong, M. G.; Costa, M.; Andrews, P. R.; Beart, P. M. Receptor site topographies for PCP-like and σ drugs: predictions from quantitative conformational, electrostatic potential, and radioreceptor analyses. *Mol. Pharmacol.* **1988**, *34*, 863–879.
(18) Van de Waterbeemd, H.; Tayar, N. E.; Testa, B.; Wikström, H.; Largent, B. Quantitative structure-activity relationships and eudismic analysis of the presynaptic dopaminergic activity and dopamine D_2 and σ receptor affinities of 3-(3-hydroxyphenyl)-piperidines and octahydrobenzo[f]quinolines. *J. Med. Chem.* **1987**, *30*, 2175–2181.
(19) Glennon, R. A.; Smith, J. D.; Ishmaiel, A. M.; El-Ashmawy, M.; Battaglia, G.; Fischer, J. B. Identification and exploitation of the σ-opiate pharmacophore. *J. Med. Chem.* **1991**, *34*, 1094–1098.
(20) Glennon, R. A.; Ishmaiel, A. M.; Smith, J. D.; Yousif, M.; El-Ashmawy, M.; Herndon, J. L.; Fischer, J.; BurkeHowie, K.; Server, A. C. Binding of substituted and conformationally restricted derivatives of N-(3-phenyl-N-propyl)-1-phenyl-2-aminopropane at σ receptors. *J. Med. Chem.* **1991**, *34*, 1855–1859.

(21) Booth, R. G.; Wyrick, S. D.; Baldessarini, R. J.; Kula, N. S.; Myers, A. M.; Mailman, R. B. A new sigma-like receptor recognized by novel phenylaminotetralins: ligand binding and functional studies. *Mol. Pharmacol.* **1993**, *44*, 1232–1239.
(22) Wyrick, S. D.; Booth, R. G.; Myers, A. M.; Owens, C. E.; Kula, N. S.; Baldessarini, R. J.; McPhail, A.; Mailman, R. B. Synthesis and pharmacological evaluation of 1-phenyl-3-amino-1,2,3,4-tetrahydronaphthalenes as ligands for a novel receptor with sigma-like neuromodulatory activity. *J. Med. Chem.* **1993**, *36*, 2542–2551.
(23) Wyrick, S. D.; Booth, R. G.; Myers, A. M.; Kula, N. S.; Baldessarini, R. J. Synthesis of [N-C^3H_3]-*trans*-(±)-1-phenyl-3-dimethylamino-6-chloro-7-hydroxy-1,2,3,4-tetrahydronaphthalene (PAT-6). *J. Labelled Compds. Radiopharm.* **1992**, *31*, 871–874.
(24) Wyrick, S. D.; Myers, A. M.; Booth, R. G.; Kula, N. S.; Baldessarini, R. J. 1-Phenyl-3-amino-1,2,3,4-tetrahydronaphthalenes and related derivatives as ligands for the neuromodulatory σ_3 receptor. Further structure-activity relationships. *J. Med. Chem.* **1994**, to be submitted for publication.
(25) Wyrick, S. D.; Myers, A. M.; Booth, R. G.; Kula, N. S.; Baldessarini, R. J.; Owens, C. E.; Mailman, R. Synthesis of [N-C^3H_3]-*trans*-(1*R*,3*S*)-(−)-1-phenyl-3-dimethylamino-1,2,3,4-tetrahydronaphthalene (H_2-PAT). *J. Labelled Compds. Radiopharm.* **1994**, *34*, 131–134.
(26) Martin, Y. C.; Bures, M. G.; Dahaner, E. A.; DeLazzer, J.; Lico, I.; Pavlik, P. A. A fast approach to pharmacophore mapping and its application to dopaminergic and benzodiazepine agonists. *J. Comput.-Aided Mol. Des.* **1993**, *7*, 83–102.
(27) Charlfson, P. S.; Bowen, J. P.; Wyrick, S. D.; Hoffman, A. J.; Cory, M.; McPhail, A. T.; Mailman, R. B. Conformational analysis and molecular modeling of 1-phenyl, 4-phenyl, and 1-benzyl-1,2,3,4-tetrahydronaphthalenes as D_1 dopamine receptor ligands. *J. Med. Chem.* **1989**, *32*, 2050–2058.
(28) Waller, C. L.; Wyrick, S. D.; Kemp, W. E.; Park, H. M.; Smith, F. T. Conformational analysis, molecular modeling, and quantitative structure-activity relationship studies of agents for the inhibition of astrocytic chloride transport. *Pharm. Res.* **1994**, *11*, 47–53.
(29) Minor, D. L.; Wyrick, S. D.; Charifson, P. S.; Mooney, D. H.; Nichols, D.; Mailman, R. B. Synthesis and molecular modeling of 1-phenyl-1,2,3,4-tetrahydroisoquinolines and the related 5,6,8,9-tetrahydro-13bH-dibenzo[*a*,*h*]quinolizines as D_1 dopamine antagonists. *J. Med. Chem.* In Press.
(30) Cramer, R. D.; Bunce, J. D.; Patterson, D.; Frank, I. E. Crossvalidation, bootstrapping, and partial least squares compared with multiple regression in conventional QSAR studies. *Quant. Struct.-Act. Relat.* **1988**, *7*, 18–25.
(31) Glennon, R. A.; Ablordeppey, S. Y.; Ismaiel, A. M.; El-Ashmawy, M. B.; Fischer, J. B.; Howey, K. B. Structural features important for σ_3 receptor binding. *J. Med. Chem.* **1994**, *37*, 1214–1219.
(32) Wold, S.; Ruhe, A.; Wold, H.; Dunn, W. The covariance problem in linear regression. The partial least squares (PLS) approach to generalized inverses. *SIAM J. Sci. Stat. Comp.* **1984**, *5*, 735–743.